MC Simulations of Gas-Liquid Transitions & Phase Equilibria

BERN01

Student: Simona Anghelina

In this project, Monte Carlo (MC) simulations are used to study the behavior of gases and liquids, particularly focusing on how they transition between each other and achieve equilibrium at different temperatures and pressures.

1. Metropolis Monte Carlo Simulations – Theory

The **Metropolis algorithm** is a way of efficiently simulate a system of particles, where the states are distributed according to the **Boltzmann distribution** (i.e., states with lower energy are more likely).

Pairwise Additivity

In most molecular simulations, the **interaction energy** between particles is calculated using pairwise additivity. This means one calculates the energy for each pair of particles using a potential, like the **Lennard-Jones potential**:

$$U(r^N) = \sum_{i=1}^{N-1} \sum_{k=i+1}^{N} \Phi(r_i, r_k) \qquad (1)$$

where U – total energy, ϕ – interparticle pair potential, N – number of particles.

Model Potentials

In real life, interactions between particles are complex and quantum mechanical in nature. However, for simulations, one often uses simpler classical potentials. For instance, all atoms interact via an attractive dispersion interaction at long range, and a repulsive exchange repulsion at short range.

One popular choice is the "*Lennard-Jones*" (L-J) potential (eq. 2), which models the interaction between neutral atoms.

$$\Phi(r) = 4\epsilon\left[\left(\frac{\sigma}{r}\right)^{12} - \left(\frac{\sigma}{r}\right)^{6}\right] \quad (2)$$

- ϵ controls the depth of the potential well, or how strong the interaction is.
- r represents distance.
- σ represents the distance at which the potential between the particles is zero.
- The first term $\left(\frac{\sigma}{r}\right)^{12}$ represents repulsion when the particles are very close.
- The second term $\left(\frac{\sigma}{r}\right)^{6}$ represents attraction at moderate distances.

The potential is illustrated in Fig. 1 below:

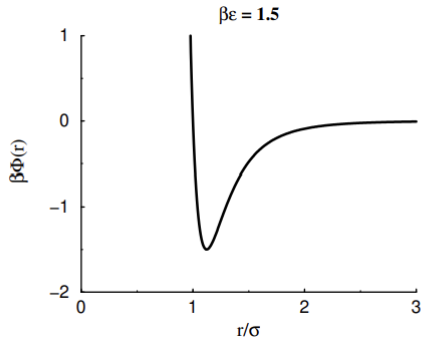

Fig. 1 – The Lennard-Jones potential.

It shows a gradual weakening at long distances and also has a strong repulsion when the atoms come very close to each other.

Periodic Boundary Conditions

In simulations, one cannot work with an infinite number of particles, so one simulates a small box of particles and replicate it infinitely in all directions. This is called **Periodic Boundary Conditions** (PBCs) which is used during the energy calculations. When a particle leaves one side of the box, it reappears on the opposite side, and it interacts with the closest copy of any other particle.

This trick removes the unrealistic boundary effects one would get with a small system and makes it behave more like a bulk material.

Energy Conservation

To make sure the simulation is working correctly, we occasionally checked that the total energy is conserved (or behaves as expected). Every time one wants to perform this step, the total interaction energy should be recalculated which should match the current energy of the system. This step is implemented in the main loop of the simulation.

An acceptable discrepancy is $\left|\frac{\delta U}{U}\right| \approx 10^{-11}$ or less. This is a good way to catch any errors in the code.

Ensembles and Macroscopic Constraints

In simulations, one can control different macroscopic variables to model real-life systems. These different constraints define different ensembles.

The project uses **the canonical ensemble (NVT)** for equilibration step, which means that the number of particles (N), volume (V), and the temperature (T) are constant, and the **isobaric ensemble (NpT**) for simulation of gas-liquid transitions and phase equilibria, which means that pressure (p), temperature (T), and number of particles (N) are fixed during the simulation. However, the volume (V) can change to allow the system to explore different densities.

Coexistence and Phase Separation

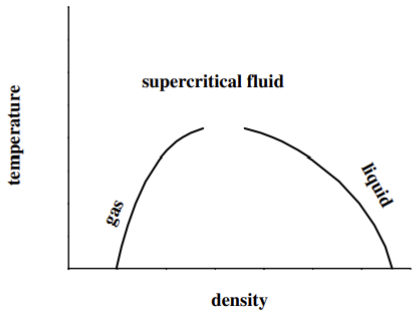

Fig. 2 – A typical gas-liquid phase diagram.

When one looks at gases and liquids, they can coexist under certain conditions. For example, in a cup of water, both liquid water and water vapor (gas) exist at the same time. This is called phase coexistence, and it happens when the pressure and temperature are just right.

If one plots how temperature and density change, it gets something called a phase diagram (Fig. 2). On this diagram, one can see regions where the system behaves like a gas, regions where it behaves like a liquid, and places where both phases coexist.

As temperature increases, the densities of the gas and liquid get closer. At a certain critical temperature, the two phases become indistinguishable, forming what's known as a supercritical fluid – state where gas and liquid no longer separate.

In this project, one will explore how gas and liquid coexist at a specific reduced temperature (a temperature normalized with respect to the interaction strength (ϵ), which is $T^* = \frac{1}{1.05} \sim 0.952$.

The goal is to simulate the gas and liquid phases separately and study their behavior. If the system's average density falls between the densities of the gas and liquid phases, it will spontaneously separate into gas and liquid regions.

Coexistence Conditions for an L-J Fluid with $\frac{\epsilon}{k_B T} = 1.05$

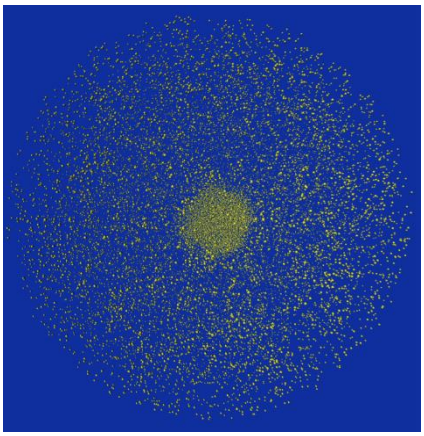

Fig. 3 – Snapshot of the "L-J fluid in a glass sphere" simulation

(provided in the project notes).

For guidance purposes, some initial simulations have been done at a reduced temperature is $T^* = \frac{1}{1.05} \sim 0.952$ and $\epsilon = 1.05$. In these simulations, a Lennard-Jones fluid was confined in a glass sphere (Fig. 3). Inside this sphere, phase separation occurs naturally, with a liquid droplet forming in the center and gas surrounding it.

These simulations produced density profiles that describe how the number of particles per unit volume changes from the center of the sphere to the edges. Here is what was found:

- The liquid phase has a density of around $n\sigma^3 \approx 0.73 - 0.74$.
- The gas phase has a much lower density, around $n\sigma^3 \approx 0.026 - 0.027$.
- The system's pressure is estimated to be, around $\beta P \sigma^3 \approx 0.023$, where $\beta = \frac{1}{k_B T}$.

However, these simulations require a large system (about 20,000 particles) to properly observe phase separation, making them computationally demanding. Using a smaller system might not work because the cost of creating a gas-liquid interface (the boundary between phases) becomes too high.

The Algorithm in Practice

Equilibration step – NVT Ensemble:

1. Initialize the System
    - Initialize particle positions randomly inside the simulation box.
    - Compute the initial energies using L-J potential.
2. Perform Monte Carlo Particle Moves (for each step in the simulation):
    - Select a random particle to move.
    - Propose a random displacement for the selected particle.
    - Ensure that particles that move outside the simulation box are wrapped back into the box using PBCs.
    - Compute the energy difference ($\Delta \mathrm{E}$) between the new state (after moving the particle) and the current state (before the move).
    - Metropolis criterion: Accept the move if $\Delta \mathrm{E} < 0$ (energy decreases), otherwise, accept the move with probability $e^{-\beta \Delta E}$.

These steps outline how the NVT Monte Carlo simulation works to maintain constant number of particles (N), constant volume (V), and constant temperature (T) while equilibrating the system and ensuring stability through periodic energy checks.

Simulation in NpT Ensemble:

In this part, the NpT ensemble uses the equilibrated positions and the corresponding energy to start with. The particle movement has been performed in 90% of the simulation time and the volume fluctuations in 10% of the simulation time.

1. Perform Monte Carlo Particle Moves (as above).
2. Perform Monte Carlo Volume Fluctuation:
    - Propose a random volume change (ΔV).
    - Reject the new volume if it is negative.
    - Compute the new box's length, rescale the positions of the particles accordingly.
    - Compute the energy difference (ΔE) using attraction and repulsion energy changes based on the new volume.
    - Metropolis criterion: Accept the volume change if $\Delta E < 0$, otherwise, accept it with probability $e^{(N \cdot \ln(\frac{Vnew}{Vold}) - \Delta E - P\Delta V)}$
3. Periodically (once in 10,000 steps), check energy conservation by comparing the current total energy with the recalculated total energy.
4. Additionally, 10 times during the simulation, the radial distribution function is constructed. At the end of the simulation, it is normalized and plotted.

These steps outline how the NPT Monte Carlo simulation maintains constant number of particles (N), constant pressure (P), and constant temperature (T). Both particle and volume moves are essential in this ensemble to allow fluctuations in volume, and energy checks ensure the stability and accuracy of the simulation.

2. Results

NPT simulations for Gas & Liquid Phases (10^6 attempted configurations)

Parameters:

$$N = 1000, \sigma = 1, k_B = 1, p = 0.023, \epsilon = 1.05, T^* = \frac{k_B T}{\epsilon} = \frac{1}{1.05} = 0.952, V_g \approx 37037, V_l \approx 1351$$

Before running the NpT simulation, we first performed a canonical NVT simulation to achieve equilibrium for both the positions and energies. The plots (Fig. 4a-d) below show how the energy stabilizes for both the gas and liquid phases. Initially, the energies start with large values but gradually decreases. By the end of the simulation, the energies become negative, with liquid phase (green line) having more negative values compared to the gas phase.

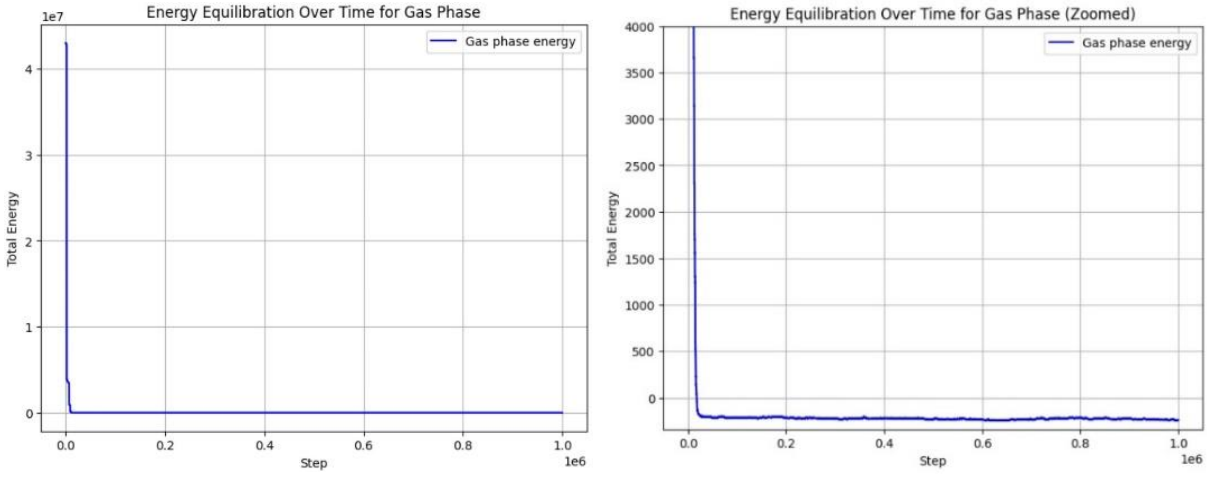

a)

b)

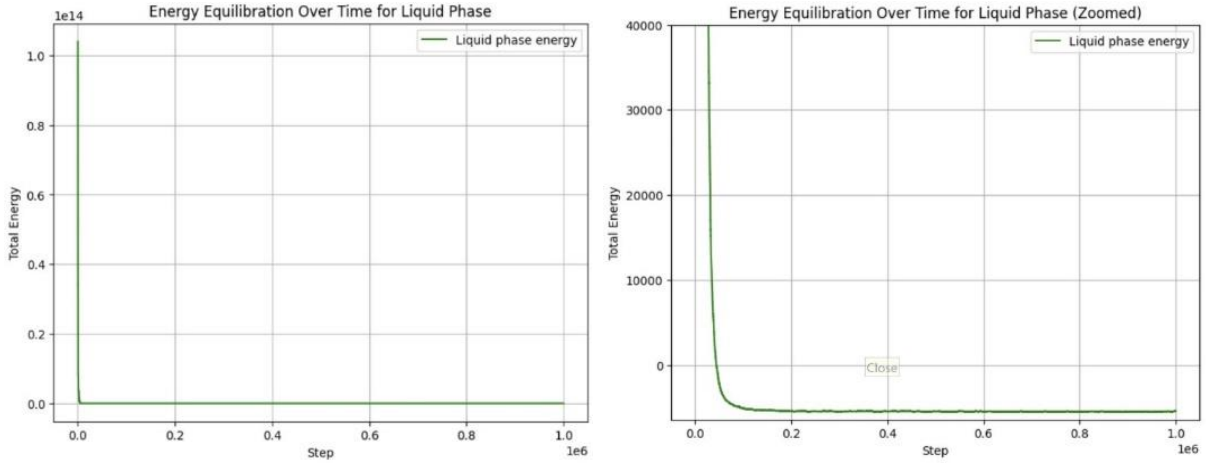

c)

d)

Fig. 4 – Energy stabilization during 10^6 attempted configurations.

a) Gas Phase (blue)
b) Gas phase Zoomed on lower energies (blue)
c) Liquid phase (green)
d) Liquid Phase Zoomed on lower energies (green)

After equilibration, the resulting positions and energies were used as inputs for the NpT simulation. The following plots present the resulting volume distributions (Fig. 5a-c), density distributions (Fig. 6a-c), and radial distributions (Fig. 7a-b).

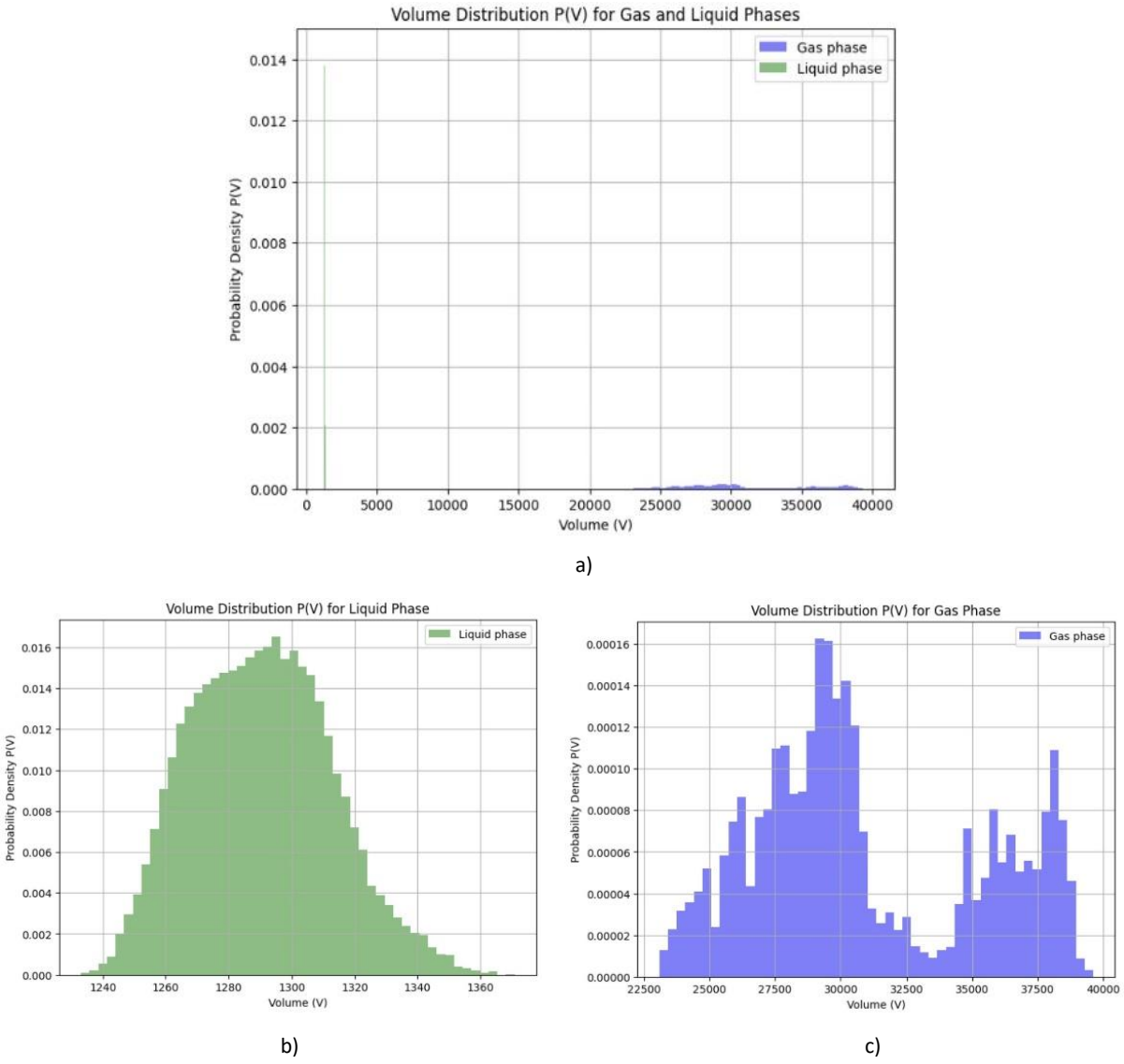

Fig. 5 – Volume Distributions after 10^6 attempted configurations.

a) Gas (blue) & Liquid (green) Phases.
b) Liquid Phase
c) Gas Phase.

As seen in Fig. 5c, the volume distribution for gas (blue) occurs at larger volumes, while for liquid (green) Fig. 5b, it appears at smaller volumes. This can be explained by the nature of intermolecular forces: in the gas phase, the forces between particles are much weaker compared to those in the liquid phase. Consequently, it is more difficult to change the volume of a liquid, while volume changes in the gas phase are more easily accepted.

In this model, the concept of intermolecular forces is represented by the Lennard-Jones potential, which makes volume changes in the liquid phase less likely to be accepted.

We also plotted the corresponding density distributions for the two phases (Fig. 6a-c), with a clear and intuitive difference: the gas phase (Fig. 6b) exhibits lower density compared to the liquid phase (Fig. 6c). Upon zooming in on the density distribution plots, it can be observed that the gas density mainly falls within range [0.025, 0.0425], while the liquid density is within the range [0.73, 0.81]. These values are consistent with the densities demonstrated in the L-J fluid example above.

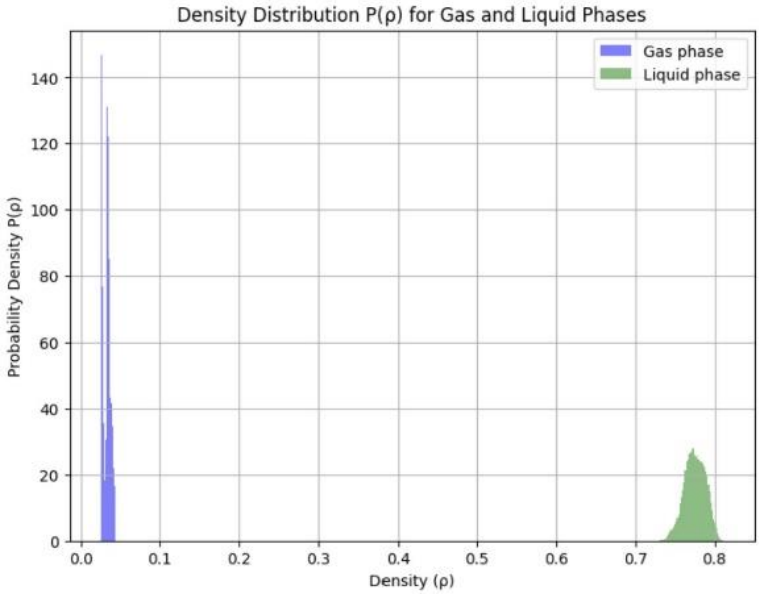

a)

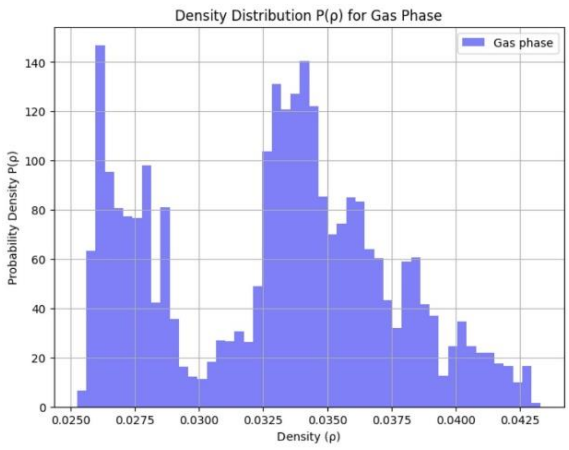

b)

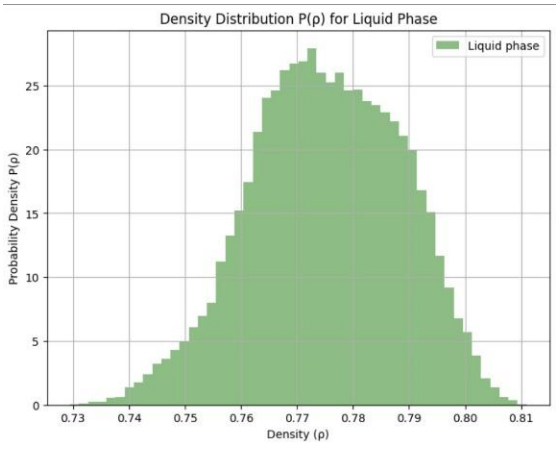

c)

Fig. 6 – Density Distributions after 10^6 attempted configurations.

a) Gas (blue) & Liquid (green) Phases.
b) Gas Phase.
c) Liquid Phase.

$< \frac{1}{V} > = 2.797\text{e} - 05$; $\quad \frac{1}{<V>} = 2.791\text{e} - 05$ – gas phase

$< \frac{1}{V} > = 0.000769$; $\quad \frac{1}{<V>} = 0.000769$ – liquid phase

In the gas phase, the particles are much farther apart, and the intermolecular forces are very weak, therefore it allows the gas particles to move freely, resulting in low density. In contrast, in the liquid phase, the intermolecular forces between particles are much stronger. The particles are closer to each other in a more condensed arrangement. As a result, liquids have a higher density.

For both phases, the values of the average of the inverse volume and the inverse of the average volume have been obtained (Fig. 6). The difference highlights the fact that volume fluctuations are more significant in the gas phase, compared to the liquid phase. In the gas phase, the values are smaller, reflecting the larger overall volumes and weaker interactions, while in the liquid phase, the values are larger due to smaller volumes and stronger interactions between particles.

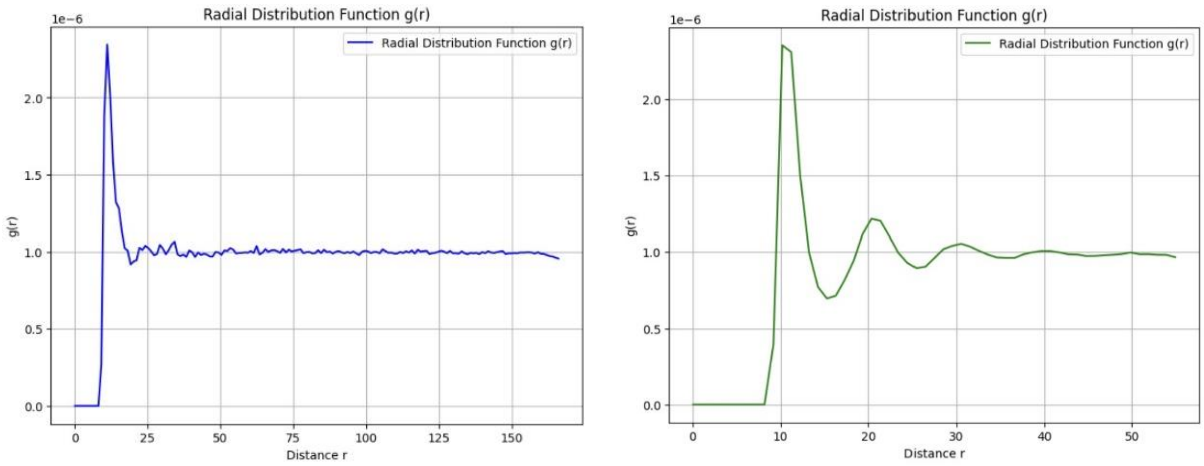

a) b)

Fig. 7 – Radial Distribution Function after 10^6 attempted configurations.

a) Gas Phase.
b) Liquid Phase

The radial distribution function $g(r)$ is plotted for both the gas (Fig. 7a) and liquid (Fig. 7b) phases. As the distance r from a particle increases, the function approaches 1.

In the gas phase, $g(r)$ quickly stabilizes to 1 after a small peak, signifying weaker interactions between particles and a more uniform distribution over larger distances. In contrast, the liquid phase shows more pronounced peaks before approaching 1, which reflects the presence of stronger intermolecular forces and structure in the liquid. These features are characteristic to the more ordered arrangement of particles in a liquid compared to gas.

NPT simulation of Gas Phase but with smaller systems (10^6 attempted configurations)

Parameters:

$N = 100\ \&\ 10, \sigma = 1, k_B = 1, p = 0.023, \epsilon = 1.05, T^* = 0.952, V_g \approx 37037.$

Additional simulations were performed on the gas phase with different particle counts (N = 100 and N = 10), and the density distributions for N = 1000, 100, and 10 were plotted for comparison in Fig. 8.

For N = 1000, the distribution shows a narrow peak at higher densities, indicating a more sharply defined density due to larger system size. For N = 100, the density remains similar, but the peak is a bit broader, reflecting larger fluctuations and higher error due to the smaller system size. For N = 10, the peak is even wider, illustrating the increased variability and uncertainty in density measurement for very small systems.

However, there is a limitation in the appearance of the results because the simulations were performed with only 10^6 steps due to RAM constraints. If the simulations could have been extended to 10^8 steps, the distributions would likely have appeared more refined, especially with a more pronounced difference between distributions of N = 1000 and N = 100.

Additionally, the results are influenced by the random number generation. In Fig. 8a, we observe a more accurate representation of the peaks at the same density, while Fig. 8b more clearly illustrates the difference in the width of the peaks.

For N = 1000, <1/V> and 1/<V> the values are very close to each other, indicating a more stable system with less variability in volume. In larger systems, the fluctuations in volume tend to average out.

For N = 100, there is a slightly larger difference between the values, reflecting an increase in volume fluctuations. As the system size decreases, these fluctuations become more pronounced.

For N = 10, the largest difference is observed. This highlights how smaller systems are more sensitive to changes, which can affect the accuracy of density-related measurements.

a)

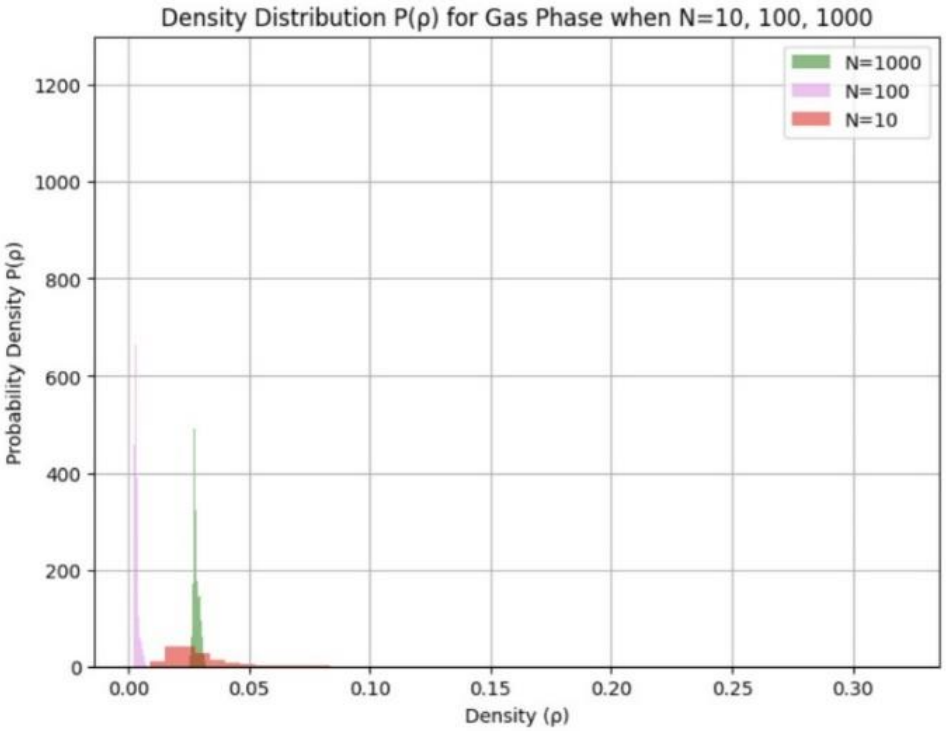

b)

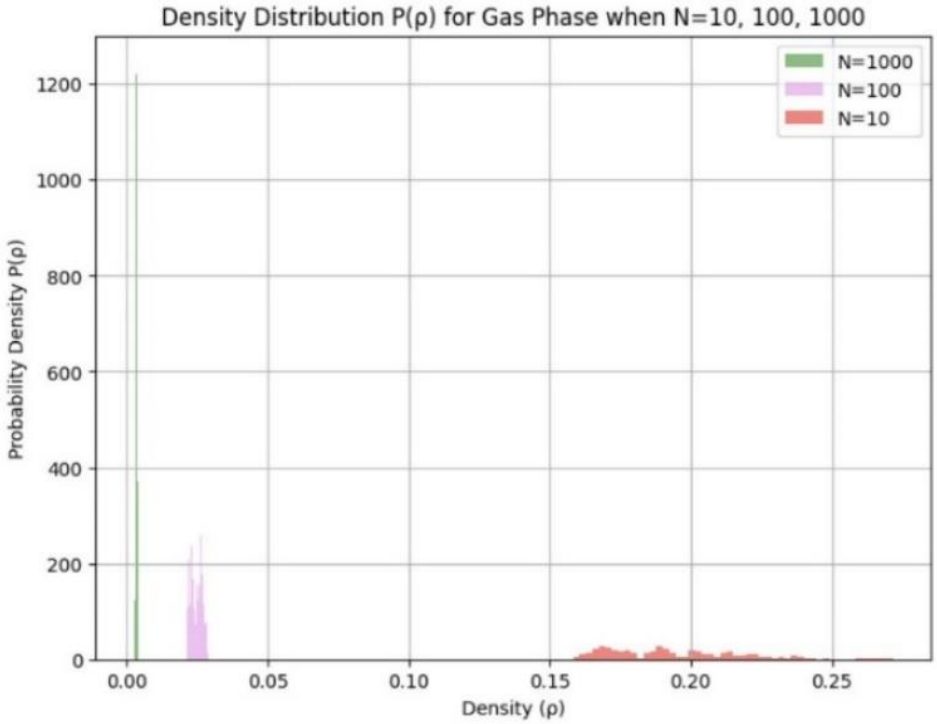

Fig. 8 – Density Distributions for N = 1000, 100 & 10 after 10^6 attempted configurations.

a) Simulation 1; b) Simulation 2.

N = 1000 -> $< \frac{1}{V} > = 2.797\text{e} - 05$; $\frac{1}{<V>} = 2.791\text{e} - 05$.

N = 100 -> $< \frac{1}{V} > = 0.000323$; $\frac{1}{<V>} = 0.000305$.

N = 10 -> $< \frac{1}{V} > = 0.00296$; $\frac{1}{<V>} = 0.00245$.

NPT simulation- Transition of Gas to Liquid phase (10^6 attempted configurations)

Parameters:

$N = 100\,, \sigma = 1, k_B = 1, \epsilon = 1.05, p = 0.023 \cdot 40 = 0.92 = , T^* = 0.952, V_g \approx 37037.$

In Fig. 9, we illustrate the phase transition from gas to liquid. Initially, the system starts in the gas phase, with a corresponding gas-phase volume, but the pressure is increased by 40 times, from 0.023 to 0.92. This significant increase in pressure triggers a phase transition from gas to liquid.

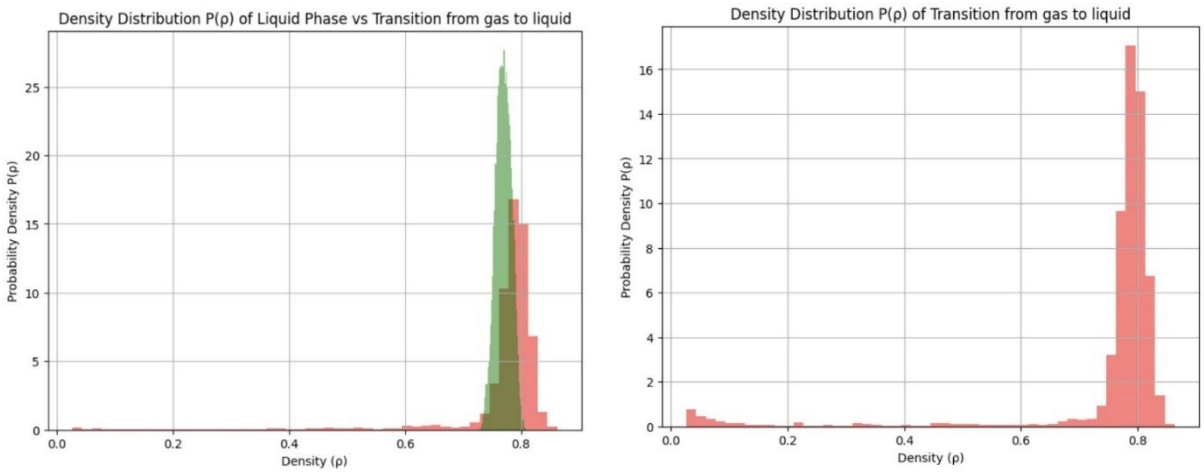

a) b)

Fig. 9 – Density Distribution of the system with N = 100 & pressure increased 40 times after 10^6 attempted configurations.

a) Liquid Phase (green) vs Transition Gas->Liquid (red).
b) Transition Gas->Liquid.

N = 100, p=0.92 -> $< \frac{1}{V} > = 0.00767;\ \frac{1}{<V>} = 0.00677.$

In Fig. 9a, the green peak, representing the initial liquid phase, overlaps with the red peak corresponding to the phase transition. This overlap clearly indicates the occurrence of the phase transition. Additionally, in Fig. 9b, the red trace left by the phase transition provides further evidence that the system has undergone a change from gas to the liquid phase. The trace reflects the system's transitions through different states during the process.

The values of <1/V> and 1/<V> during the phase transition suggest that there is a slight difference between the average inverse volume and the inverse of the average volume.

In general, <1/V> tends to be larger than 1/<V>, especially during transitions where significant fluctuations occur. This indicates that during the transition, the system experiences more variations in volume, which is characteristic of a phase change. The fluctuation in volume reflects the system's adjustment to the increasing pressure, making the volume distribution less uniform during the transition phase.

NPT simulation- Transition of Gas to Liquid phase (10^6 attempted configurations)

Parameters:

$N = 1000\,, \sigma = 1, k_B = 1, p = 0.923, \epsilon \approx 0.775\,, T^* \approx 1.32, \epsilon \approx 0.775, V_g \approx 37037.$

For this simulation at critical temperature of 1.32 and pressure 0.923, the volume distributions were plotted for the initial gas and liquid phases, as well as for the gas phase at critical temperature (Fig. 10a-b).

a)

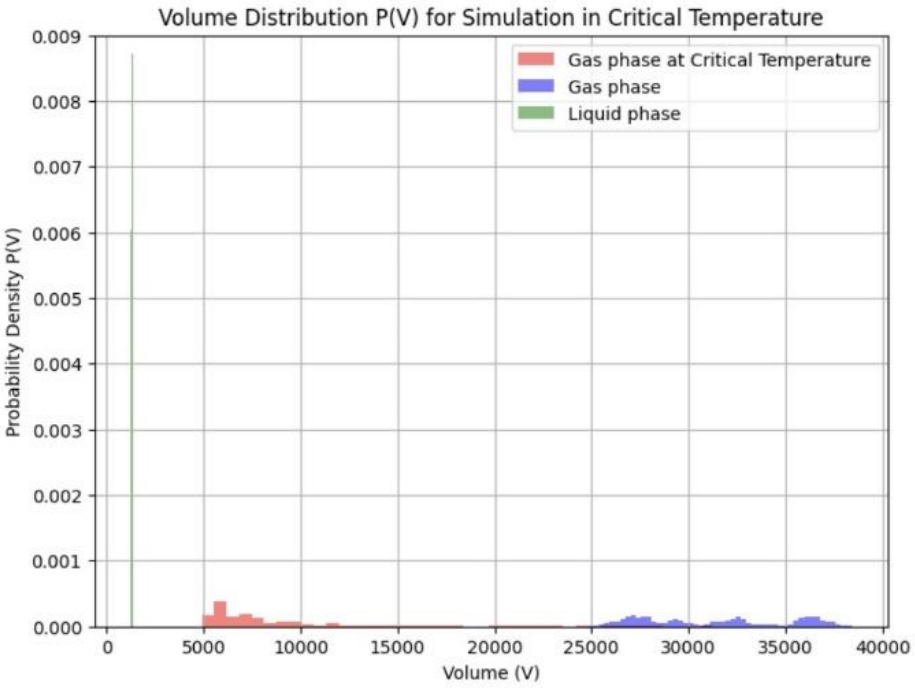

b)

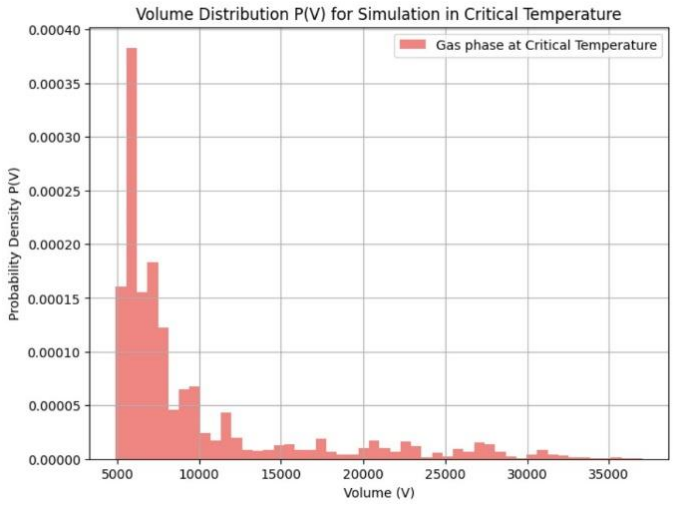

Fig. 10 – Volume Distributions after 10^6 attempted configurations.

a) Gas (blue), Liquid (green) Phases & Gas at Critical Temperature (red).
b) Gas at Critical Temperature.

From these plots, it can be observed that the volume distribution for the gas phase at critical temperature (shown in red) has a wide range of values, indicating that the system is fluctuating between gas and liquid-like behaviors. The volume distributions for the initial gas (blue) and liquid (green) phases show distinct peaks, with the gas phase having higher volumes and the liquid phase much smaller volumes. This confirms that, at critical temperature, the system exhibits characteristics of both phases, signaling a transition region. The broader distribution for the gas at critical temperature reflects the system's fluctuations, where no clear boundary between phases is present.

If the simulation were run under the same conditions with N = 100.000, we would expect more accurate and well-defined distributions that reflect phase behaviors more clearly. At critical temperature, fluctuations in volume are large as the system transitions between gas and liquid phases. With a larger N, the fluctuations might be captured more clearly with reduced noise, providing a more accurate representation of the phase transition.

Conclusions

In this project, we successfully simulated both gas and liquid phases using Lennard-Jones potential in the canonical (NVT) and isobaric (NpT) ensembles. By first equilibrating the system in the NVT ensemble, we ensured that the particle configurations and energies stabilized before proceeding to the NpT simulations, where volume fluctuations were introduced.

Key insights from the simulations include:

1. **Volume and Density Distributions**: The simulations clearly show distinct volume and density distributions for the gas and liquid phases. Gas, with its weaker intermolecular forces, exhibited a broader volume distribution, while the liquid phase, characterized by stronger intermolecular forces, maintained a more stable, narrower volume range. Density distributions reflected similar trends, with has densities being much lower and more variable than those of the liquid phase.
2. **Radial Distribution Function**: The radial distribution functions for both phases revealed important structural information. In both gas and liquid phases, the function $g(r)$ approached 1 at larger distances, indicating that at grater separations, the particles are distributed uniformly.
3. **Effects of System Size**: We explored simulations with different particle numbers (N = 1000, 100 & 10). As expected, larger systems produced more refined distributions, while smaller systems exhibited broader peaks due to the noise. A larger system size, such as N = 100.000, would likely provide even more accurate and smoother distributions, though at the cost of greater computational resources.
4. **Phase Transition**: We induced a phase transition by increasing the pressure, resulting in a gas transitioning into a liquid-like state. The density distribution for gas phase after the transition closely overlapped with that of the liquid phase, indicating the system's shift towards a denser configuration. The presence of residual traces from the gas phase post-transition confirms the transition process.

The simulations demonstrate the powerful ability of molecular dynamics to capture and visualize phase behaviours in gas and liquid. They provide valuable insights into the nature of intermolecular forces and how they influence macroscopic properties like density and volume. This study also highlights the importance of system size and simulation parameters in achieving accurate representations of physical phenomena.